

Quantum Dynamics of the Avian Compass

Zachary B. Walters¹

¹*Max Planck Institute for Physics of Complex Systems,
Nöthnitzer Strasse 38, D-01187 Dresden, Germany*

(Dated: August 4, 2021)

The ability of migratory birds to orient relative to the Earth’s magnetic field is believed to involve a coherent superposition of two spin states of a radical electron pair. However, the mechanism by which this coherence can be maintained in the face of strong interactions with the cellular environment has remained unclear. This Letter addresses the problem of decoherence between two electron spins due to hyperfine interaction with a bath of spin 1/2 nuclei. Dynamics of the radical pair density matrix are derived and shown to yield a simple mechanism for sensing magnetic field orientation. Rates of dephasing and decoherence are calculated *ab initio* and found to yield millisecond coherence times, consistent with behavioral experiments.

The ability of a migratory bird to orient itself relative to the Earth’s magnetic field is at once a familiar feature of everyday life and a puzzling problem of quantum mechanics. That birds have this ability is well established by a long series of behavioral experiments. However, the precise mechanism by which an organism may sense the orientation of the weak geomagnetic field remains unclear and theoretically problematic.

Although commonly referred to as the “avian compass,” an ability to sense the local magnetic field orientation has been observed in every major group of vertebrates, as well as crustaceans, insects, and a species of mollusc [1, 2]. For the majority of species, the primary compass mechanism appears to be light-activated, with a few exceptions such as the sea turtle or the subterranean mole rat[2]. In addition to a light-activated compass located in the eye, migratory birds are believed to possess a separate mechanism involving magnetite, with possible receptors identified in the beak[3], the middle ear[4] and the brain stem[5], although the existence of a receptor in the beak has been challenged in a recent study[6]. This paper addresses the light-activated mechanism, which in addition to being widespread is also well studied by a long series of behavioral experiments, reviewed in [2, 7–10].

The basic parameters of the compass mechanism may be probed by confining a bird in a conical cage during its preferred migration period [11]. The restless nocturnal hopping behavior, or *Zugunruhe*, will tend to orient in the preferred migration direction, and the effects of environmental parameters can be judged by whether they affect the bird’s ability to orient. Such experiments have established that the compass is light activated, with an abrupt cutoff between wavelengths 560.5 and 567.5 nm [12], and that birds are sensitive to the orientation of magnetic field lines but not their polarity – they cannot distinguish magnetic north from south[13]. Provocatively, a recent experiment has found that an oscillatory magnetic field oriented transverse to the static field can cause disorientation when it is narrowly tuned to the Larmor frequency for an electron in the static field to flip its spin. On resonance, an oscillatory field strength of 15 nT

(Rabi frequency $\Omega_{\text{Rabi}} = 1320$ Hz) is sufficient to cause disorientation[14, 15].

Qualitatively, such experiments are well explained by a “radical pair” model of the avian compass[16, 17], also known as the Ritz model. Here, an asymmetry $\Delta\mu = \mu_1 - \mu_2$ in the coupling of the magnetic field to the two electrons, arising due to chemical or physical properties of the receptor, allow the magnetic field to drive coherent oscillations between the $|s, m_s\rangle = |0, 0\rangle$ singlet state $|s\rangle$ and the $|s, m_s\rangle = |1, 0\rangle$ triplet state $|t\rangle$ of an electron radical pair formed by absorption of a photon. If the singlet and triplet states react to form distinguishable byproducts, or can be otherwise distinguished[18], monitoring the ratio of the byproducts probes the time spent in each state, and thus the oscillation frequency. Use of a radical pair is a common denominator in a wide variety of biological processes sensitive to magnetic fields, recently reviewed in [19].

The radical pair model gives an excellent phenomenological description of the avian compass, and predicts disorientation by an on-resonance oscillatory field. However, it remains theoretically problematic, requiring that coherence be maintained between different spin states for very long times despite the presence of an environment which is very hostile to this. As observed in [20], the slow spin flip time ($\pi/\Omega_{\text{Rabi}} = 3\text{ms}$) implies that the process it disrupts must be slower still. [20] and [21–23] use similar methods to infer coherence times of $10^{-5} - 10^{-4}\text{s}$. However, the proteins and water molecules present in a cellular environment possess large numbers of hydrogen nuclei, each of which interact with the radical pair via the hyperfine interaction. Somehow, the necessary quantum information must survive such interactions long enough to give a biologically useful signal.

Previous work considering the radical pair compass in the presence of decoherence includes [24–27], treating effects of rapid singlet and triplet reaction rates on the evolution of the density matrix. Decoherence due to hyperfine interactions has been treated in terms of an effective magnetic field in [28], while [29–31] consider a radical pair interacting with a small number of nuclei.

The related problem of decoherence in a singlet/triplet quantum dot has been treated in [32, 33].

This paper gives an analytic treatment of the preservation and decay of coherence for a radical pair interacting with a bath of spin 1/2 nuclei. A long lived component of the quantum information is identified, and shown to yield a simple and robust compass mechanism. Design considerations for an efficient compass are identified, and the coherence lifetime is shown to be consistent with lifetimes inferred from behavioral experiments. Atomic units are used throughout.

To maximize readability, the text of this paper is split into two parts. The body of the paper addresses the classic Ritz model of the radical pair compass with the addition of decoherence terms which are included as Lindblad superoperators. Because the Ritz model addresses only dynamics within the two state $m_z = 0$ subspace of the radical pair, only these two states are included. The Ritz model assumes that the two electrons experience a slightly different Zeeman coupling to the local magnetic field; as the receptor or receptors involved in the avian compass are currently unknown, this paper incorporates this assumption without proof. Both the eigencomponents of dephasing induced by the hyperfine interaction and their rates of decay are derived in the technical appendix, which includes all four states of the radical pair, plus two states of the nuclear spin. The asymmetric Zeeman coupling assumed by the Ritz model is not included in the derivation of dephasing rates, but could readily be added using the same approach.

The evolution of the reduced density matrix ρ for a radical pair interacting with a Markovian bath is given by the Lindblad master equation

$$\frac{\partial}{\partial t}\rho = i[H_0^{rp}, \rho] + \sum_{\kappa} \Gamma_{\kappa} \mathcal{L}_{\kappa}[\rho], \quad (1)$$

Here

$$H_0^{rp} = \bar{\mu}(\vec{s}_1 + \vec{s}_2) \cdot \vec{B} + \Delta\mu(\vec{s}_1 - \vec{s}_2) \cdot \vec{B} \quad (2)$$

is the Zeeman Hamiltonian, and

$$\mathcal{L}_{\kappa}[\rho] = -\rho L_{\kappa}^{\dagger} L_{\kappa} - L_{\kappa}^{\dagger} L_{\kappa} \rho + 2L_{\kappa} \rho L_{\kappa}^{\dagger} \quad (3)$$

is the Lindblad superoperator corresponding to projection operator $L_{\kappa} = |\kappa\rangle\langle\kappa|$. The difference $\Delta\mu$ in the magnetic susceptibilities of the two electrons is assumed to arise due to short range interactions with the receptor molecule[31, 34, 35]; as the receptor or receptors involved in the avian compass are as yet unknown,[36–38], this paper simply assumes a value of $\Delta\mu \approx 1$ without derivation.

If all Lindblad operators in Eq. 1 were zero, the equation would recover the Ritz model of the avian compass, in which decoherence is ignored. Following the Ritz model, theoretical treatments of the avian compass have frequently assumed that rates of decay are slow relative to

the dynamics induced by the Zeeman Hamiltonian. However, as shall be shown here, the limit of rapid dephasing also allows for an efficient compass, with a reaction product signal which is relatively easy and unambiguous to interpret.

As derived in the appendix, hyperfine interactions between the electronic spins of the radical pair and the nuclear spins of atoms in the surrounding environment – most plentifully, hydrogen atoms in the surrounding water molecules – causes a loss of coherence between spin states of the radical pair. Although both the singlet and the triplet state have total spin $m_s = 0$, the hyperfine interaction couples the triplet state to other triplet states with $m_s = \pm 1$, while the singlet state is not coupled to any other states. Because of this, the spin state of the radical pair becomes entangled with the unobserved spin states of the bath nuclei, and coherence between different states of the radical pair decays with time.

At the same time that coherence decays due to hyperfine interaction with the bath, it is being created by the normal Hamiltonian evolution which arises when two states are connected by a matrix element. The evolution of the density matrix includes both effects, and in the limit that the decay rate is very large, they become very closely balanced against each other for a particular component of the density matrix, which accordingly decays very slowly. Because the other components of the density matrix decay rapidly, the density matrix describing the radical pair soon evolves to consist of only the long lived component. As will be seen, the rate of decay for this long lived component gives all the information necessary for an efficient chemical compass. Because this decay manifests itself as a transfer of population from the singlet to the triplet state, it is well suited to detection by spin selective chemical reactions which create different sets of byproducts depending on whether the radical pair is in the triplet or singlet state.

As derived in the appendix, the rates of decay relevant to the avian compass are given by two parameters, which can be found analytically. In Eq. 1, $\Gamma_{|s\rangle} = \Gamma_{|t\rangle} = \bar{\Gamma}/2$ and $\Gamma_{|\uparrow\downarrow\rangle} = \Gamma_{|\downarrow\uparrow\rangle} = \Delta\Gamma/2$, where $\bar{\Gamma}$ is large for moderate field strengths and $\Delta\Gamma$ is zero for some orbital symmetries. Mapping the density matrix to a Bloch sphere according to $(\rho_{ss} - \rho_{tt}) \rightarrow (\rho_{01} + \rho_{10}) = x\sigma_x$, $(\rho_{st} - \rho_{ts}) \rightarrow (\rho_{10} - \rho_{01}) = iy\sigma_y$, and $(\rho_{st} + \rho_{ts}) \rightarrow (\rho_{00} - \rho_{11}) = z\sigma_z$, where $\sigma_{x,y,z}$ are Pauli matrices, it can be seen that a Lindblad operator corresponding to projecting the Bloch vector in one direction causes decay of vectors perpendicular to that direction, while the difference in magnetic susceptibilities $\Delta\mu$ causes the Bloch vector to precess about the z axis when a magnetic field is present, thereby creating coherence between $|s\rangle$ and $|t\rangle$. In the Bloch sphere picture, a quantum mechanically pure state corresponds to a vector with length 1, while a completely incoherent state corresponds to a vector of length 0. Hamiltonian evolution rotates the Bloch vector

about some axis, while dephasing causes some components of the vector to decay. In the work that follows, it is useful to draw a distinction between the rate of *dephasing* – the rate at which these components would decay if there were no Hamiltonian evolution, and the rate of *decoherence* – the rate at which the length of the Bloch vector decays when both dephasing and Hamiltonian evolution are taken into account. As will be seen, a large rate of dephasing may paradoxically lead to a small rate of decoherence. This is the quantum mechanical version of Zeno’s paradox, and is appropriately known as the quantum Zeno effect[24, 27, 39].

The evolution of the density matrix components can be found analytically by calculating the evolution due to H and $\bar{\Gamma}$ in a basis where singlet and triplet states form the $\pm z$ axes in the Bloch sphere, then transforming to a basis where $|\uparrow\downarrow\rangle$ and $|\downarrow\uparrow\rangle$ make up the z axis to include the effects of $\Delta\Gamma$. As in [40], differential equations for the density matrix components due to H and $\bar{\Gamma}$ are given by

$$\begin{aligned} \frac{d^2}{dt^2}(\rho_{ss} - \rho_{tt}) + \bar{\Gamma} \frac{d}{dt}(\rho_{ss} - \rho_{tt}) + (B_z \Delta\mu)^2(\rho_{ss} - \rho_{tt}) &= 0 \\ \frac{d^2}{dt^2}(\rho_{ts} - \rho_{st}) + \bar{\Gamma} \frac{d}{dt}(\rho_{ts} - \rho_{st}) + (B_z \Delta\mu)^2(\rho_{ts} - \rho_{st}) &= 0 \\ \frac{d}{dt}(\rho_{ts} + \rho_{st}) &= -\bar{\Gamma}(\rho_{ts} + \rho_{st}) \\ \frac{d}{dt}(\rho_{ss} + \rho_{tt}) &= 0, \end{aligned} \quad (4)$$

where ρ_{ss} gives the population of singlet states, ρ_{st} is a coherence term between singlet and triplet, and so on.

In Eq. 4, $(\rho_{ss} - \rho_{tt})$ and $(\rho_{ts} - \rho_{st})$ behave as damped harmonic oscillators, with time dependence $P(t) = Ae^{\lambda_+ t} + Be^{\lambda_- t}$, where

$$\lambda_{\pm} = \frac{-\bar{\Gamma} \pm \sqrt{\bar{\Gamma}^2 - 4(B_z \Delta\mu)^2}}{2}. \quad (5)$$

In the limit that $\bar{\Gamma} \gg |2B_z \Delta\mu|$, the system is strongly overdamped and the coherence terms will decay much more slowly than the base rate of dephasing, $\bar{\Gamma}$. In the Bloch sphere picture, the z component of the Bloch vector decays rapidly, while the x and y components decay slowly. It is this slow loss of coherence, shown in Figure 1, which allows for a biologically useful signal.

Although arising from a different source, these dynamics are similar to the quantum Zeno regime treated in [24, 27], where fast singlet or triplet reaction rates take the place of rapid dephasing, and to [40], where the long lived coherences occur in photosynthetic molecules. Because the z component of the Bloch vector decays rapidly, the symmetry group of the long lived information is $U(1)$ rather than $SU(2)$.

The value of $\bar{\Gamma} = \frac{5}{3}B\Delta\mu N_{\text{sphere}}$ derived in the appendix can be found for a cellular environment by assuming a density of hydrogen nuclei equal to that of liquid

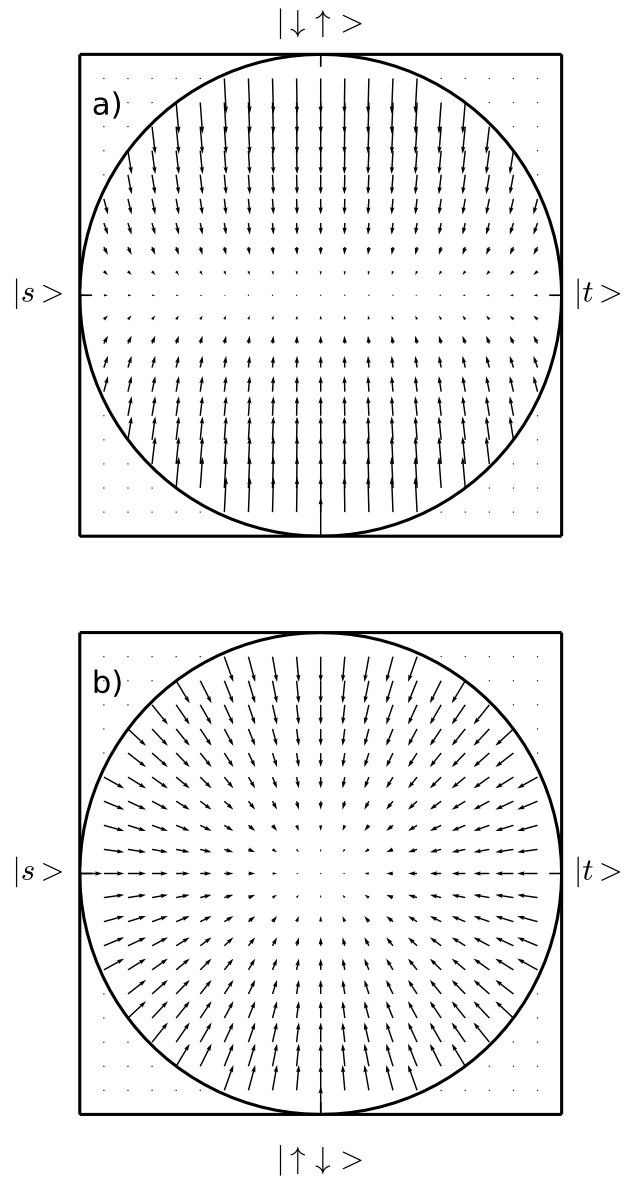


FIG. 1. Decoherence of the Bloch vector, $\vec{V}_B(\vec{x})$, in the xz plane for an efficient and an inefficient compass molecule. The z component decays as $e^{-\bar{\Gamma}t}$, the x as $e^{-\lambda_+ t}$. a) $\frac{\bar{\Gamma}}{B\Delta\mu} = 8.5$, $\frac{\Delta\Gamma}{B\Delta\mu} = 6 \times 10^{-4}$, contrast=0.99. b) $\frac{\bar{\Gamma}}{B\Delta\mu} = 8.5$, $\frac{\Delta\Gamma}{B\Delta\mu} = 5.8$, contrast=0.01. For both plots, a small value of $\bar{\Gamma}$ has been used to accentuate the decay of the x component.

water. For $B=50 \mu\text{T}$, $N_{\text{sphere}} = 3300$ is the number of nuclei within radius $r_0 = 43$ bohr, at which the hyperfine interaction equals the Zeeman interaction in magnitude. The dynamics are thus strongly overdamped, with a dephasing lifetime $\bar{\Gamma}^{-1} = 43$ ps and a coherence lifetime $\tau = \lambda_+^{-1} = 1.3$ ms, somewhat longer than the 10^{-4} s- 10^{-6} s inferred in [20, 21].

The dynamics of the overdamped radical pair model

depart in an essential way from those of the Ritz model, or from a model in which dephasing is present but weak. Because the decay of the Bloch vector is overdamped, it does not precess about the z axis as in the original radical pair model. Rather, a vector in the equatorial plane is frozen in place and evolves only through decoherence. For an initially pure singlet state, $\rho(0) = \begin{pmatrix} 1/2 & 1/2 \\ 1/2 & 1/2 \end{pmatrix}$ in the $|\uparrow\downarrow\rangle, |\downarrow\uparrow\rangle$ basis, so that $\dot{\rho} = -1/2 \begin{pmatrix} 0 & \lambda_+ + \Delta\Gamma \\ \lambda_+ + \Delta\Gamma & 0 \end{pmatrix}$, or $1/2 \begin{pmatrix} -\lambda_+ - \Delta\Gamma & 0 \\ 0 & \lambda_+ + \Delta\Gamma \end{pmatrix}$ in the $|s\rangle, |t\rangle$ basis. Loss of coherence thus manifests itself as a transfer of population from singlet to triplet at a rate which varies as $B^2 \cos^2 \theta$. Identical logic applies if the initial state is a triplet. As this rate of population transfer contains the necessary directional information, a chemical compass requires only that the state which is not originally populated (here, the triplet) have a reaction rate sufficiently large to prevent backwards population transfer. Population transfer due to $\Delta\Gamma$, which does not depend on the orientation of the molecule, decreases the sensitivity of the compass by decreasing contrast between orientations with a high rate of transfer and orientations with a slow rate. Assuming that the triplet reaction rate is sufficiently high to prevent backwards population transfer, the ratio of triplet to singlet byproducts is

$$R_{ts}(\theta) = \frac{\lambda_+ + \Delta\Gamma}{k_s} \approx \frac{|B\Delta\mu \cos \theta|^2}{\bar{\Gamma}k_s} + \frac{\Delta\Gamma}{k_s}, \quad (6)$$

where k_s is the singlet reaction rate. Note that a simple consequence of this model is that the chemical compass is insensitive to the difference between positive and negative values of $B \cos \theta$ – ie, it is insensitive to the difference between magnetic North and South. This is consistent with behavioral experiments, in which the inclination of field lines to the horizon, rather than their polarity, determines the preferred migratory direction.

While the identity of the avian compass receptor remains unknown, a number of design considerations may be inferred from Eq. 6 and from the dephasing dynamics derived in the appendix.

One such consideration relates to the mechanism of detecting the formation of triplet states. While the original radical pair model proposed a spin sensitive chemical reaction, this is not an essential feature of the model, and more recent papers [18] have proposed that physical detection of the triplet states may be advantageous. A possible mechanism for such detection can be seen in Table III in the appendix, which shows that dephasing due to nuclei distant from the radical pair will result in population transfer from state $|t\rangle$ to states $|t^\pm\rangle$, with lifetime 33 ps. As the $m_s = \pm 1$ states have nonzero magnetic moments, they are easily distinguishable from the $m_s = 0$ states by physical means. Because equilibration between

the populations of states $|t\rangle$, $|t^+\rangle$ and $|t^-\rangle$ is rapid, detection of any triplet state will suffice for the purposes of the compass mechanism.

Second, it can be seen that the sensitivity of the compass mechanism depends greatly upon the form taken by the dephasing superoperators. An upper limit for the sensitivity of the compass mechanism may be found by considering the contrast between North/South and East/West alignment

$$\text{contrast} = \frac{R_{ts}(0) - R_{ts}(\pi/2)}{R_{ts}(0) + R_{ts}(\pi/2)} = \frac{(B_0\Delta\mu)^2}{2\Delta\Gamma\bar{\Gamma} + (B_0\Delta\mu)^2}. \quad (7)$$

Here the contrast is independent of k_s and k_t , depending only upon the ratio of $\bar{\Gamma}\Delta\Gamma$ and $(B\Delta\mu)^2$. Figure 1 illustrates the decay of the Bloch vector for both an efficient (high contrast) and an inefficient (low contrast) compass. As $\bar{\Gamma}$ is large relative to $B\Delta\mu$, it follows that an efficient compass receptor must have $\Delta\Gamma$ small or zero.

From table V in the appendix, it can be seen that $\Delta\Gamma$ will be small only in the case that it is zero by symmetry. Here the rate of dephasing $\frac{5\alpha\kappa}{6\beta}$ due to $\vec{I} \cdot \Delta\vec{S}$ for a nucleus far from the radical pair is inversely proportional to $\tau_\epsilon = 1/\kappa$, the rate of decay for correlations in the environment. Thus, it is likely that an efficient compass will employ an excited state with cylindrical symmetry, which eliminates this term.

Similar logic can be used to compare the loss of contrast resulting from an oscillatory field tuned to the Larmor frequency with that seen in behavioral experiments. Here the oscillatory field may flip the spin of one electron in the radical pair, thereby populating states with $m_s = \pm 1$. As the populations of $|t^+\rangle$, $|t^-\rangle$ and $|t\rangle$ equilibrate rapidly, the final triplet populations will be indistinguishable from those produced by the compass mechanism. As derived in the appendix, the rate of such spin flips is $\Omega = \frac{|B_{\text{osc}}|}{2\sqrt{2}}$. Adding this rate to $R_{ts}(\theta)$ and setting $\Delta\Gamma = 0$ yields a new equation for the contrast

$$\text{contrast} = \frac{B^2\Delta\mu^2}{B^2\Delta\mu^2 + |B_{\text{osc}}|\bar{\Gamma}/\sqrt{2}}, \quad (8)$$

which is plotted as a function of B_{osc} in Figure 2. Consistent with [15], Figure 2 shows a rapid loss of contrast as B_{osc} grows from 1 to 10 nT – precisely the range in which experiment shows a crossover from oriented to disoriented behavior. Some inconsistency with experiment can be seen if the static field strength is doubled – while experiment shows disoriented behavior for $(B, B_{\text{osc}}) = (100 \mu\text{T}, 15 \text{ nT})$ and oriented behavior for $(50 \mu\text{T}, 5 \text{ nT})$, Figure 2 shows higher contrast for the first case than for the second.

When the static field is doubled in the absence of an oscillatory field, behavioral experiments [41] show temporary disorientation lasting less than an hour, indicating that the biological signal is affected by the field strength, but the ability to orient is not. Here the contrast in Eq.

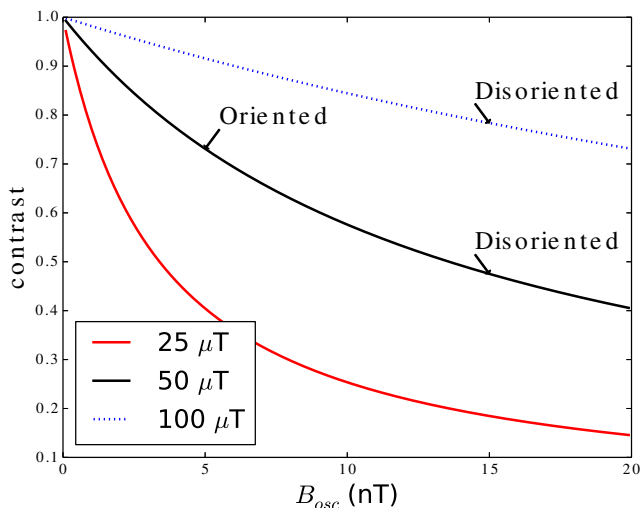


FIG. 2. (Color online) Contrast between North/South and East/West alignment using Eq. 8. Geomagnetic field strength in Hamburg, Germany is $47 \mu\text{T}$. Consistent with [14], a rapid loss of contrast occurs as B_{osc} increases from 1 to 10 nT.

7 is unaffected by the change in field strength, while the visibility $R_{ts}(0) - R_{ts}(\pi/2)$ depends on the ratio of B to k_s . For a migratory bird, which is exposed to a range of field strengths, it may thus be advantageous to have some means of controlling k_s , so that the same receptor could give usable visibility at a variety of field strengths.

The avian compass described in this paper represents a unique example of a quantum mechanical process which not only survives but is actually sustained by interaction with a surrounding bath. Through use of a radical pair, it is similar to a wide range of biological processes affected by a magnetic field, including processes as significant as ATP synthesis and DNA replication by polymerases [19]. Although the precise identity of the receptor or receptors involved in the avian compass remains unknown, simple geometrical assumptions allow information sufficient for numerical comparison with experiment to be derived from first principles. The proposed mechanism requires neither unique properties nor elaborate manipulation of the radical pair state, and the biologically observable signal is distinctive and easy to interpret. The avian compass thus represents a simple model system for the emerging and still largely unexplored role of quantum mechanics in biological processes.

Appendix: Dephasing Rates

The decoherence of a spin system due to interactions with a surrounding spin bath is one of the central theoretical problems associated with the avian compass. It is also a longstanding open problem in its own right [42].

This appendix section considers the decay of density matrix components arising due to hyperfine interactions between two spin 1/2 electrons and a surrounding bath of spin 1/2 nuclei. Dephasing due to the bath is treated within the Born-Markov approximation – the spin state of each nucleus is assumed to be in thermal equilibrium with the rest of the bath, to bear no memory of the previous states of the system or the bath, and to cause decoherence in the central spin system independently of the other nuclei in the bath. Having found rates of decay due to individual nuclei, rates due to the bath as a whole are found by performing a volume integral over all space assuming a constant density of nuclei per unit volume.

The hyperfine interaction between a single nucleus and a radical electron pair is given by

$$V_{\text{HF}} = \sum_{i,k} \left(\frac{2\mu_I}{I} \frac{1}{|r_{ik}|^3} \right) (\vec{I}_k \cdot \vec{S}_i - 3(\vec{I} \cdot \hat{r})(\vec{S} \cdot \hat{r})), \quad (9)$$

where the r^{-3} dependence of the hyperfine interaction means that distant electrons interact with effectively distinct reservoirs, while proximate electrons interact with the same nuclei with comparable strength. As selection rules will be important in this derivation, note that the $I = 1/2$ nuclear spin has different angular character than an $l = 1$ magnetic vector field, so that the spin states coupled in this treatment may differ from effective field approaches.

Dephasing in the interaction picture

The hyperfine interaction between a nucleus and a radical pair contains several terms with different symmetries, each of which causes the density matrix to evolve in different ways. In addition, the system evolves due to the Zeeman interaction with the magnetic field. In view of the large size (8×8) of the matrices involved in these calculations, it is much simpler to treat the decoherence induced by each term separately.

The decay of the density matrix due to the combination of the Zeeman term and each of the three hyperfine terms will be found in two limits – one in which the hyperfine term acts as a perturbation to the Zeeman term, one in which the Zeeman term acts as a perturbation to the hyperfine term. Writing the full Hamiltonian $H = H_0 + V$ as the sum of a dominant term H_0 and a perturbative term V , the evolution of the density matrix can be calculated in the interaction picture. For nuclei close to the radical pair, H_0 is the hyperfine term and V is the Zeeman term, and vice versa for distant nuclei.

Working in the interaction picture,

$$\begin{aligned} \frac{\partial}{\partial t} \rho_{i,k,\epsilon;i k',\epsilon'}^I(t) = \\ - \int_0^\infty d\Delta t [V^I(t), [V^I(t - \Delta t), \rho_{i,k,\epsilon;i k',\epsilon'}^I(t - \Delta t)]], \end{aligned} \quad (10)$$

where over short times

$$\rho^I(t + \Delta t) = e^{-iH_0\Delta t} e^{iH\Delta t} \rho^I(t) e^{-iH\Delta t} e^{iH_0\Delta t} \quad (11)$$

and

$$V(t + \Delta t) = e^{-iH_0\Delta t} V e^{iH_0t}. \quad (12)$$

Here i indexes electronic states, k nuclear states, and ϵ the states of the nucleus's local environment. Rather than calculate e^{iHt} directly, which would require diagonalizing H anew for every value of α/β , the Hamiltonian exponential is approximated by the split operator method [43]

$$e^{iH\Delta t} = e^{iH_0\Delta t/2} e^{iV\Delta t} e^{iH_0\Delta t/2} + \mathcal{O}(\Delta t^3), \quad (13)$$

so that

$$\begin{aligned} \rho^I(t + \Delta t) \approx \\ e^{-iH_0\Delta t/2} e^{iV\Delta t} e^{iH_0\Delta t/2} \rho^I(t) e^{-iH_0\Delta t/2} e^{-iV\Delta t} e^{iH_0\Delta t/2}. \end{aligned} \quad (14)$$

The integrand of Eq. 10 is now given by the product of a large number of matrix exponentials multiplying the density matrix, so that each element of $\dot{\rho}^I$ is given by a semi-infinite integral time integral of a large number of Fourier components. These integrals can be evaluated by imposing the Born and Markov approximations, so that

$$\text{Tr}_{\epsilon=\epsilon'} \rho_{i,k,\epsilon;i k',\epsilon'}^I(t + \Delta t) = \rho_{i,k;i k'}^I(t + \Delta t) \delta(\Delta t) \delta_{k,k'} P_k, \quad (15)$$

and $\dot{\rho}_{i,k,i';k'}^I = 0$ if $k \neq k'$, so that both ρ^I and $\dot{\rho}^I$ are diagonal with respect to the nuclear spin state. Here the Markov approximation is imposed by multiplying the integrand by a delta function inside the time integral, rather than simply replacing $\rho(t + \Delta t)$ with $\rho(t)$ as in [44].

The time integrals over the various Fourier components can now be evaluated using a dimensionless integral. Setting $\delta(x) = \lim_{\nu \rightarrow \infty} \nu e^{-\nu x}$, where ν and x are dimensionless,

$$\int_0^\infty dt e^{i\omega t} \delta(t) = \lim_{\nu \rightarrow \infty} \frac{1}{\omega} \int_0^\infty dx e^{ix} \nu e^{-\nu x} = \frac{1}{\omega}. \quad (16)$$

In the limit that $e^{i\omega t}$ oscillates slowly relative to the timescale τ on which the bath becomes Markovian, the above integral becomes

$$\int_0^\infty dt e^{i\omega t} \delta(t) = \lim_{\nu \rightarrow \infty} \frac{1}{\kappa} \int_0^\infty dx e^{i\omega x/\kappa} \nu e^{-\nu x} = \frac{1}{\kappa}, \quad (17)$$

where $\kappa = \tau^{-1}$. Here, Eq. 16 is used for integrals over oscillating Fourier terms in Eq. 10, while Eq. 17 is used for integrals over constant terms.

Having found $\dot{\rho}^I$ in terms of ρ^I , the decaying components of the density matrix and their associated decay rates may be found by solving an eigenvalue equation. For the terms involving $\vec{I} \cdot (\vec{S}_1 \pm \vec{S}_2)$, tables III, IV, V, and VI give these rates to second order in α and first order in β for both the symmetric and the antisymmetric hyperfine components, in the limits that $\alpha \ll \beta$ and $\beta \ll \alpha$.

Matrix forms for the hyperfine and Zeeman interaction

In order to evaluate Eq. 10, it is necessary to have matrix forms for H_0 and V . Here it is convenient to decompose the full hyperfine interaction into three terms, of the form $\vec{I} \cdot (\vec{S}_1 \pm \vec{S}_2)$, and $(\vec{I} \cdot \hat{r})(\vec{S} \cdot \hat{r})$. As each of these terms have different symmetry, they will cause decay among different eigencomponents of the density matrix.

Terms involving $\vec{I} \cdot (\vec{S}_1 \pm \vec{S}_2)$ For the terms involving $\vec{I} \cdot \vec{S}$, rather than treating the interactions between the nucleus and each electron separately, it is convenient to reexpress Eq. 9 in terms of the sum $\vec{S} = \vec{S}_1 + \vec{S}_2$ and the difference $\Delta\vec{S} = \vec{S}_1 - \vec{S}_2$ of the two spins. If the distance $|\vec{R}_k|$ between the radical pair and a particular nucleus k is large relative to the spatial extent of the radical pair and the distance between the two electrons, the hyperfine interaction with that nucleus can be broken up into two components having different angular character. Writing the spatial coordinates of the electrons as $\vec{r} = (\vec{r}_1 + \vec{r}_2)/2$ and $\Delta\vec{r} = (\vec{r}_1 - \vec{r}_2)/2$ and assuming that $|\vec{R}_k| \gg |\vec{r}|$ and $|\vec{R}_k| \gg |\Delta\vec{r}|$, the hyperfine interaction with each nucleus k can be written as the sum of a symmetric term and an antisymmetric term

$$V_{\text{HF}}(\vec{R}_k, \vec{r}, \Delta\vec{r}) = \sum_k V_{\text{HF}}^{(S)}(\vec{R}_k, \vec{r}, \Delta\vec{r}) + V_{\text{HF}}^{(A)}(\vec{R}_k, \vec{r}, \Delta\vec{r}) \quad (18)$$

where to leading order in the small parameters $|\vec{r}|$ and $|\Delta\vec{r}|$

$$V_{\text{HF}}^{(S)}(\vec{R}_k, \vec{r}, \Delta\vec{r}) = \sum_k \left(\frac{2\mu_I}{I|\vec{R}_k|^3} \right) \vec{I}_k \cdot \vec{S} \quad (19)$$

and

$$V_{\text{HF}}^{(A)}(\vec{R}_k, \vec{r}, \Delta\vec{r}) = \sum_k \left(\frac{3\mu_I \Delta\vec{r} \cdot \vec{R}_k}{I|\vec{R}_k|^5} \right) \vec{I}_k \cdot \Delta\vec{S}. \quad (20)$$

Note that $|s\rangle$ and $|t\rangle$ are eigenstates of $\vec{S} = \vec{S}_1 + \vec{S}_2$, with eigenvalues $|\bar{s}, \bar{m}\rangle = |0, 0\rangle$ and $|1, 0\rangle$, while states $|\uparrow\downarrow\rangle$ and $|\downarrow\uparrow\rangle$ are eigenstates of $\Delta\vec{S} = \vec{S}_1 - \vec{S}_2$ with eigenvalues $|\Delta s, \Delta m_s\rangle = |1, \pm 1\rangle$.

Integrating over the spatial component of the wavefunction now leaves the hyperfine interaction in the form of a spin operator, and the coefficients of the dot products in Eqs. 19 and 20 as functions of the nuclear coordinates alone. Writing $V_{\text{HF}}^{(S)}(\vec{R}_k) = \sum_k \alpha(|\vec{R}_k|) \vec{I}_k \cdot \vec{S}$ and $V_{\text{HF}}^{(A)}(\vec{R}_k) = \sum_k \alpha(|\vec{R}_k|, \theta_k) \vec{I}_k \cdot \Delta \vec{S}$, where θ_k is the angle between \vec{R}_k and $\Delta \vec{r}$,

$$\begin{aligned} \alpha(|\vec{R}_k|) &= \int d^3 \vec{r} \int d^3 \Delta \vec{r} \varphi^*(\vec{r}, \Delta \vec{r}) \frac{2\mu_I}{I|\vec{R}_k|^3} \varphi(\vec{r}, \Delta \vec{r}) \\ &= \frac{2\mu_I}{I|\vec{R}_k|^3} \end{aligned} \quad (21)$$

If $\varphi(\vec{r}, \Delta \vec{r}) = \bar{\varphi}(\vec{r}) \Delta F(\Delta r) Y_{l_o, m_o}(\Delta \Omega)$ is separable, with well defined l_o and m_o ,

$$\begin{aligned} \alpha(|\vec{R}_k|, \theta_k) &= \int d^3 \vec{r} \int d^3 \Delta \vec{r} \\ &\varphi^*(\vec{r}, \Delta \vec{r}) \frac{3\mu_I |\Delta \vec{r}| |\vec{R}_k| \cos(\theta_k)}{I|\vec{R}_k|^5} \varphi(\vec{r}, \Delta \vec{r}) \\ &= \frac{3\mu_I |\widetilde{\Delta \vec{r}}| \widetilde{\cos(\theta_k)}}{I|\vec{R}_k|^4}, \end{aligned} \quad (22)$$

where $|\widetilde{\Delta \vec{r}}| = \langle \varphi | |\Delta \vec{r}| | \varphi \rangle$ and $\widetilde{\cos(\theta_k)} = \langle \varphi | \cos(\theta_k) | \varphi \rangle$. Note that the $\cos(\theta_k)$ integral introduces a selection rule. Recalling that $\cos(\theta_k)$ has angular character $l = 1$, with m_l dependent upon the orientation, the Wigner-Eckart theorem gives

$$\widetilde{\cos(\theta_k)} = \langle l_o || T^1 || l_o \rangle \langle l_o m_o 1 m_l | l_o m_o \rangle \quad (23)$$

where $\langle l_o || T^1 || l_o \rangle$ is a reduced matrix element and $\langle l_o m_o 1 m_l | l_o m_o \rangle = \frac{m_o}{\sqrt{l_o(l_o+1)}}$ if $m_l = 0$ and $l_o \geq 1/2$, but 0 otherwise. Setting $m_o = 0$ eliminates this term by symmetry.

Having performed these integrals, matrix elements for both components of the hyperfine interaction have the form $\alpha(\vec{R}_k) \vec{I}_k \cdot \vec{S}$, where $\vec{S} = \vec{S}$ for the symmetric component and $\vec{S} = \Delta \vec{S}$ for the antisymmetric component. Matrix elements of the dot product can be evaluated using a Clebsch-Gordan expansion ([45] Eq. 9.33)

$$\begin{aligned} \langle s' m'_s I' m'_I | \vec{I} \cdot \vec{S} | s m_s I m_i \rangle &= \\ &\sum_{J=|s-I|}^{s+I} \sum_{M=-J}^J \langle s' m'_s I' m'_I | J M \rangle \langle s m_s I m_i | J M \rangle \times \\ &\frac{1}{2} (J(J+1) - s(s+1) - I(I+1)) \delta_{s,s'} \delta_{I,I'} \end{aligned} \quad (24)$$

so that

$$\vec{I} \cdot \vec{S} = \begin{pmatrix} 0 & 0 & 0 & 0 & 0 & 0 & 0 & 0 \\ 0 & 0 & 0 & 0 & 0 & 0 & 0 & 0 \\ 0 & 0 & 0 & 0 & 0 & \frac{1}{\sqrt{2}} & 0 & 0 \\ 0 & 0 & 0 & 0 & 0 & 0 & \frac{1}{\sqrt{2}} & 0 \\ 0 & 0 & 0 & 0 & \frac{1}{2} & 0 & 0 & 0 \\ 0 & 0 & \frac{1}{\sqrt{2}} & 0 & 0 & -\frac{1}{2} & 0 & 0 \\ 0 & 0 & 0 & \frac{1}{\sqrt{2}} & 0 & 0 & \frac{1}{2} & 0 \\ 0 & 0 & 0 & 0 & 0 & 0 & 0 & -\frac{1}{2} \end{pmatrix} \quad (25)$$

where the bras and kets represent eigenstates with quantum numbers $|s, m_s; m_I\rangle$. Eigenkets and corresponding indices for the $\vec{S} = \vec{S}$ basis are given in Table I, and for $\vec{S} = \Delta \vec{S}$ in Table II. Here the $|\bar{s}, \bar{m}_s\rangle = |1, \pm 1\rangle$ states, although losing degeneracy with the $m_s = 0$ subspace in a nonzero magnetic field, must be included for the sake of second order terms in Eq. 10.

Term involving $(\vec{I} \cdot \hat{r})(\vec{S} \cdot \hat{r})$ The asymmetric term in the hyperfine interaction proportional to $(\vec{I} \cdot \hat{r})(\vec{S} \cdot \hat{r})$ differs qualitatively from the terms involving $\vec{I} \cdot \vec{S}$ and $\vec{I} \cdot \Delta \vec{S}$ by the presence of a quantization axis other than the one parallel to the applied magnetic field – the axis between the radical pair and the nucleus. As this paper is concerned with the decoherence between $|s\rangle$ and $|t\rangle$ defined with respect to the magnetic field axis, the operator

$$(\vec{I} \cdot \hat{r})(\vec{S} \cdot \hat{r}) = \begin{pmatrix} 0 & 0 & 0 & 0 & 0 & 0 & 0 & 0 \\ 0 & 0 & 0 & 0 & 0 & 0 & 0 & 0 \\ 0 & 0 & 0 & 0 & 0 & 0 & 0 & 0 \\ 0 & 0 & 0 & 0 & 0 & 0 & 0 & 0 \\ 0 & 0 & 0 & 0 & \frac{1}{2} & 0 & 0 & 0 \\ 0 & 0 & 0 & 0 & 0 & -\frac{1}{2} & 0 & 0 \\ 0 & 0 & 0 & 0 & 0 & 0 & -\frac{1}{2} & 0 \\ 0 & 0 & 0 & 0 & 0 & 0 & 0 & \frac{1}{2} \end{pmatrix} \quad (26)$$

defined with respect to the \hat{r} axis, with state numbering as defined in table I is rotated into the \hat{z} axis according to $R(\theta)(\vec{I} \cdot \hat{r})(\vec{S} \cdot \hat{r})R(-\theta)$, where $R(\theta)$ is the outer product of the rotation operators

$$R_{\text{nuclear}}(\theta) = \begin{pmatrix} \cos(\theta) & -\sin(\theta) \\ \sin(\theta) & \cos(\theta) \end{pmatrix} \quad (27)$$

and

$$R_{\text{electronic}}(\theta) = \begin{pmatrix} 1 & 0 & 0 & 0 \\ 0 & \cos(\theta) & -\frac{\sin(\theta)}{\sqrt{2}} & \frac{\sin(\theta)}{\sqrt{2}} \\ 0 & \frac{\sin(\theta)}{\sqrt{2}} & \frac{1}{2}(\cos(\theta) + 1) & \frac{1}{2}(1 - \cos(\theta)) \\ 0 & -\frac{\sin(\theta)}{\sqrt{2}} & \frac{1}{2}(1 - \cos(\theta)) & \frac{1}{2}(\cos(\theta) + 1) \end{pmatrix}, \quad (28)$$

the rotation operators in the nuclear and electronic bases, respectively.

The Zeeman interaction In addition to the hyperfine interaction, the system will evolve due to the influence of

the Zeeman Hamiltonian $H_z = \beta(\vec{S}_1 + \vec{S}_2)$, given by

$$H_z = \beta * \begin{pmatrix} 0 & 0 & 0 & 0 & 0 & 0 & 0 & 0 \\ 0 & 0 & 0 & 0 & 0 & 0 & 0 & 0 \\ 0 & 0 & 0 & 0 & 0 & 0 & 0 & 0 \\ 0 & 0 & 0 & 0 & 0 & 0 & 0 & 0 \\ 0 & 0 & 0 & 0 & 1 & 0 & 0 & 0 \\ 0 & 0 & 0 & 0 & 0 & 1 & 0 & 0 \\ 0 & 0 & 0 & 0 & 0 & 0 & -1 & 0 \\ 0 & 0 & 0 & 0 & 0 & 0 & 0 & -1 \end{pmatrix} \quad (29)$$

in the basis diagonalizing \vec{S} , and

$$H_z = \beta * \begin{pmatrix} 0 & 0 & 1 & 0 & 0 & 0 & 0 & 0 \\ 0 & 0 & 0 & 1 & 0 & 0 & 0 & 0 \\ 1 & 0 & 0 & 0 & 0 & 0 & 0 & 0 \\ 0 & 1 & 0 & 0 & 0 & 0 & 0 & 0 \\ 0 & 0 & 0 & 0 & 0 & 0 & 0 & 0 \\ 0 & 0 & 0 & 0 & 0 & 0 & 0 & 0 \\ 0 & 0 & 0 & 0 & 0 & 0 & 0 & 0 \\ 0 & 0 & 0 & 0 & 0 & 0 & 0 & 0 \end{pmatrix} \quad (30)$$

in the basis diagonalizing $\Delta\vec{S}$. Here the Zeeman terms involving the nuclear magneton, smaller than the Bohr magneton by a factor of m_e/m_n , have been omitted.

Integrated rates of dephasing

Eigencomponents and rates of dephasing can now be found by substituting the matrices found in the previous section into Eq. 10 using Eqs. 13, 15, 16, and 17. The resulting rates are summarized in Tables III, IV, V, and VI for hyperfine interactions of the form $\vec{I} \cdot (\vec{S}_1 \pm \vec{S}_2)$. Because the strength of the hyperfine interaction varies with the position of the nucleus within the bath, these tables give results in terms of α , the coefficient of the $\vec{I} \cdot \vec{S}$ in Eq. 25 and β , the coefficient of the matrix $(\vec{S}_1 + \vec{S}_2)$ in Eqs. 29 and 30.

The term involving $(\vec{I} \cdot \hat{r})(\vec{S} \cdot \hat{r})$ is more computationally difficult than the terms involving $\vec{I} \cdot (\vec{S}_1 \pm \vec{S}_2)$ because the decaying eigencomponents may vary as a function of the angle θ between \hat{r} and \hat{z} , the direction of the magnetic field. As this paper is primarily concerned with the decay of the ρ_{st} density matrix component, only that component of $\dot{\rho}_{st}$ proportional to ρ_{st} will be presented here. For the case when the Zeeman term acts as a perturbation to the hyperfine term, this rate is identically zero, independent of θ . For the case when the hyperfine term acts as a perturbation to the Zeeman term, this rate is given

Index	$ \bar{s}, \bar{m}_s; m_I\rangle$	$ m_{s1}m_{s2}; m_I\rangle$
1	$ 0, 0; \uparrow\rangle$	$(\uparrow\downarrow; \uparrow\rangle - \downarrow\uparrow; \uparrow\rangle)/\sqrt{2}$
2	$ 0, 0; \downarrow\rangle$	$(\uparrow\downarrow; \downarrow\rangle - \downarrow\uparrow; \downarrow\rangle)/\sqrt{2}$
3	$ 1, 0; \uparrow\rangle$	$(\uparrow\downarrow; \uparrow\rangle + \downarrow\uparrow; \uparrow\rangle)/\sqrt{2}$
4	$ 1, 0; \downarrow\rangle$	$(\uparrow\downarrow; \downarrow\rangle + \downarrow\uparrow; \downarrow\rangle)/\sqrt{2}$
5	$ 1, 1; \uparrow\rangle$	$ \uparrow\uparrow; \uparrow\rangle$
6	$ 1, 1; \downarrow\rangle$	$ \uparrow\uparrow; \downarrow\rangle$
7	$ 1, -1; \uparrow\rangle$	$ \downarrow\downarrow; \uparrow\rangle$
8	$ 1, -1; \downarrow\rangle$	$ \downarrow\downarrow; \downarrow\rangle$

TABLE I. Indices for eigenstates of $|\bar{s}, \bar{m}_s; m_I\rangle$ and the corresponding kets in the $|m_{s1}m_{s2}; m_I\rangle$ basis.

Index	$ \Delta s, \Delta m_s; m_I\rangle$	$ m_{s1}m_{s2}; m_I\rangle$
1	$ 0, 0; \uparrow\rangle$	$(\uparrow\uparrow; \uparrow\rangle - \downarrow\downarrow; \uparrow\rangle)/\sqrt{2}$
2	$ 0, 0; \downarrow\rangle$	$(\uparrow\uparrow; \downarrow\rangle - \downarrow\downarrow; \downarrow\rangle)/\sqrt{2}$
3	$ 1, 0; \uparrow\rangle$	$(\uparrow\uparrow; \uparrow\rangle + \downarrow\downarrow; \uparrow\rangle)/\sqrt{2}$
4	$ 1, 0; \downarrow\rangle$	$(\uparrow\uparrow; \downarrow\rangle + \downarrow\downarrow; \downarrow\rangle)/\sqrt{2}$
5	$ 1, 1; \uparrow\rangle$	$ \uparrow\downarrow; \uparrow\rangle$
6	$ 1, 1; \downarrow\rangle$	$ \uparrow\downarrow; \downarrow\rangle$
7	$ 1, -1; \uparrow\rangle$	$ \downarrow\uparrow; \uparrow\rangle$
8	$ 1, -1; \downarrow\rangle$	$ \downarrow\uparrow; \downarrow\rangle$

TABLE II. Indices for eigenstates of $|\Delta s, \Delta m_s; m_I\rangle$ and the corresponding kets in the $|m_{s1}m_{s2}; m_I\rangle$ basis.

to second order in α and first order in β by

$$\begin{aligned} \dot{\rho}_{st} = & \frac{\alpha^2 \sin^2(\theta) \cos^3(\theta)}{8\beta} - \frac{\alpha^2 \sin(3\theta) \sin(\theta) \cos^3(\theta)}{8\beta} \\ & + \frac{\alpha^2 \sin^4(\theta) \cos(\theta)}{8\beta} - \frac{\alpha^2 \sin(3\theta) \sin^3(\theta) \cos(\theta)}{8\beta} \\ & - \frac{\alpha^2 \sin^2(\theta) \cos^3(\theta)}{8\omega} + \frac{\alpha^2 \sin(3\theta) \sin(\theta) \cos^3(\theta)}{8\omega} \\ & - \frac{1}{4}\alpha \sin^4(\theta) \cos(\theta) + \frac{1}{4}\alpha \sin(3\theta) \sin^3(\theta) \cos(\theta). \end{aligned} \quad (31)$$

Noting that

$$\int_0^\pi \dot{\rho}_{st}(\theta) \sin(\theta) d\theta = 0, \quad (32)$$

it can be seen that the asymmetric component of the hyperfine interaction does not contribute to the decay of the singlet-triplet coherence after integrating over the volume occupied by the bath.

Volume integral over the bath For the purpose of calculating dynamics of the avian compass, two rates are particularly important, because they enter into the equations of motion for the 2×2 density matrix describing dynamics within the $|s\rangle$ and $|t\rangle$ subspace. These two rates are given by the integrals over all space of $\frac{5\alpha^2}{3\beta}$, the rate of decay for coherence terms ρ_{13} , ρ_{31} , ρ_{24} and ρ_{42} in Table III, and $\frac{20\alpha^2}{9\beta}$, the rate of decay for population imbalances

Decay Rate	Component
$-\frac{\alpha}{2}$	ρ_{82}
	$\rho_{46} + \rho_{73}$
	$\rho_{37} + \rho_{64}$
	ρ_{51}
	ρ_{28}
	ρ_{15}
$\frac{\alpha^2}{9\beta} - \frac{\alpha}{3}$	ρ_{71}
	ρ_{62}
	ρ_{26}
$-\frac{20\alpha^2}{9\beta}$	$\rho_{77} - \rho_{44}$
	$\rho_{66} - \rho_{33}$
$-\frac{5\alpha^2}{3\beta}$	ρ_{86}
	ρ_{75}
	ρ_{68}
	ρ_{57}
	ρ_{42}
	ρ_{31}
	ρ_{24}
	ρ_{13}
$-\frac{\alpha^2}{3\beta} - \frac{\alpha^2}{6\kappa} - \frac{\alpha}{18}$	ρ_{53}
	ρ_{48}
	ρ_{84}
$-\frac{40\alpha^2}{27\beta} - \frac{2\alpha}{9}$	$\rho_{73} - \rho_{46}$
	$\rho_{64} - \rho_{37}$

TABLE III. Decaying density matrix components and associated decay rates resulting from Zeeman interaction $V = H_z = \beta(S_{z1} + S_{z2})$ and hyperfine interaction $V = V_{HF} = \alpha(\vec{I} \cdot \vec{S})$ in the limit that $\alpha \ll \beta$. Indices are numbered according to Table I. Negative rates correspond to decay.

$\rho_{77} - \rho_{44}$ and $\rho_{66} - \rho_{33}$. As these rates apply when $\alpha < \beta$, the volume integral will be performed over all space outside a sphere of radius r_0 , where r_0 is the radius at which $\alpha = \beta$, where the hyperfine interaction between a nuclear and an electronic spin has magnitude equal to the interaction of the electron spin with the static magnetic field.

As these rates involve a density of nuclei multiplying a volume integral, it is helpful to parameterize the result in terms of $N_{\text{sphere}} = (N/V)\frac{4}{3}\pi r_0^3$, the number of nuclei within a radius r_0 . Here (N/V) is the density of nuclei per unit volume. Substituting $\beta = B\mu_B$, $\alpha = \alpha_0 r^{-3}$, $\alpha_0 r_0^{-3} = B\mu_B$ yields integrated rates of decay $\bar{\Gamma} = \frac{5}{3}B\mu_B N_{\text{sphere}}$ for elements ρ_{13} , ρ_{31} , ρ_{24} and ρ_{42} and $\frac{20}{9}B\mu_B N_{\text{sphere}}$ for elements $\rho_{77} - \rho_{44}$ and $\rho_{66} - \rho_{33}$.

r_0 and N_{sphere} can be found by recalling that $\alpha_0 = (2\mu_B \frac{m_e}{m_p})/I$ and $I = 1/2$, yielding $r_0 = 42$ bohr for a magnetic field of $50 \mu\text{T}$. Assuming a density of protons equal to that of liquid water yields $N_{\text{sphere}} = 3300$. Thus,

Decay Rate	Component
$-\frac{\beta}{2}$	ρ_{82}
	ρ_{51}
	ρ_{28}
	ρ_{15}
$-\frac{4\beta^2}{27\alpha} - \frac{10\beta}{9}$	ρ_{86}
	ρ_{75}
	ρ_{68}
$-\frac{\beta^2}{162\kappa} - \frac{37\beta}{81}$	$\rho_{73} - \rho_{46}$
	$\rho_{64} - \rho_{37}$
$-\frac{\beta^2}{18\kappa} - \frac{\beta}{3}$	$\rho_{73} + \rho_{46} \left(4 - \frac{\beta}{\beta - 2\kappa}\right)$
	$\rho_{64} + \rho_{37} \left(4 - \frac{\beta}{\beta - 2\kappa}\right)$
$-\frac{2\beta^2}{27\alpha} - \frac{\beta^2}{18\kappa} - \frac{\beta}{6}$	ρ_{84}
	ρ_{71}
	ρ_{62}
	ρ_{53}
	ρ_{48}
	ρ_{35}
	ρ_{26}
	ρ_{17}

TABLE IV. Decaying density matrix components and associated decay rates resulting from hyperfine interaction $H_0 = \alpha(\vec{I} \cdot \vec{S})$ and Zeeman interaction $V = H_z = \beta(S_{z1} + S_{z2})$ in the limit that $\beta \ll \alpha$. Indices are numbered according to Table I. Negative rates correspond to decay.

it is apparent that $\frac{\bar{\Gamma}}{B\mu_B} = \frac{5}{3} \cdot 3300 \gg 1$, so that the system is strongly overdamped. The timescale for decay of population imbalances $\rho_{77} - \rho_{44}$ and $\rho_{66} - \rho_{33}$ is given by $(\frac{20}{9}B\mu_B N_{\text{sphere}})^{-1} = 33$ ps, so that any population transferred to the $|s, m_s\rangle = |1, 0\rangle$ state will quickly equilibrate with the populations of states $|1, \pm 1\rangle$.

Rabi oscillation in the limit of strong dephasing

In [15], an oscillatory magnetic field tuned to the Larmor frequency for an electron in the static geomagnetic field was found to cause disorientation in European robins. In the body of the paper, this was attributed to electrons flipping their spin due to the oscillatory field, creating an alternate pathway for the formation of triplet state population from an initial singlet state which does not depend on the orientation of the compass molecule. Because the populations of triplet states $|t^+\rangle$, $|t^-\rangle$ and $|t\rangle$ equilibrate very rapidly, the population of triplet states created in this way will be indistinguishable from those created by the compass mechanism.

In the absence of dephasing, the rate of spin flips due to Hamiltonian $H = \begin{pmatrix} \frac{\omega_1}{2} & d \cos(\omega_2 t) \\ d \cos(\omega_2 t) & -\frac{\omega_1}{2} \end{pmatrix}$ is the Rabi

Decay Rate	Component
$-\frac{5\alpha}{12}$	$\rho_{46} + \rho_{73}$ $\rho_{37} + \rho_{64}$
$-\frac{\alpha^2}{2\beta}$	$\rho_{24} + \rho_{42}$ $\rho_{13} + \rho_{31}$
$-\frac{5\alpha\kappa}{6\beta}$	ρ_{86} ρ_{75} ρ_{68} ρ_{57}
$-\frac{\alpha^2}{12\kappa} - \frac{5\alpha}{18}$	ρ_{82} ρ_{15}
$-\frac{2\alpha^2}{\beta} + \frac{\alpha^2}{6\kappa} - \frac{\alpha}{9}$	$\rho_{77} - \rho_{44}$ $\rho_{66} - \rho_{33}$
$-\frac{\alpha^2}{2\beta} - \frac{5\alpha}{12}$	$\rho_{71} - \rho_{26}$ $\rho_{62} - \rho_{17}$
$-\frac{\alpha^2}{2\beta} - \frac{\alpha^2}{6\kappa} + \frac{\alpha}{9}$	$\rho_{42} - \rho_{24}$ $\rho_{31} - \rho_{13}$
$-\frac{\alpha^2}{2\beta} - \frac{7\alpha}{18}$	$\rho_{26} + \rho_{71}$ $\rho_{17} + \rho_{62}$
$-\frac{2\alpha^2}{\beta} - \frac{\alpha}{6}$	$\rho_{73} - \rho_{46}$ $\rho_{64} - \rho_{37}$
$-\frac{\alpha^2}{2\beta} - \frac{\alpha^2}{12\kappa} - \frac{5\alpha}{18}$	ρ_{84} ρ_{53} ρ_{48} ρ_{35}
$\frac{\alpha^2}{12\beta} - \frac{\alpha^2}{12\kappa} + \frac{\kappa\alpha}{36\beta} - \frac{\alpha}{36}$	ρ_{51} ρ_{28}

TABLE V. Decaying density matrix components and associated decay rates resulting from Zeeman interaction $V = H_z = \beta(S_{z1} + S_{z2})$ and hyperfine interaction $V = V_{HF} = \alpha(\vec{I} \cdot \Delta\vec{S})$ in the limit that $\alpha \ll \beta$. Indices are numbered according to Table II. Negative rates correspond to decay.

frequency $\Omega_{\text{Rabi}} = \sqrt{d^2 + \Delta^2}$, where $\Delta = \omega_2 - \omega_1$ is the detuning between the driving frequency and the spacing between the two energy levels. As shown elsewhere in this section, the dynamics of the radical pair density matrix can be greatly affected by dephasing induced by the surrounding nuclear spin bath; thus, a brief discussion of Rabi oscillation in the limit of rapid dephasing is warranted. Here the effects of dephasing are given by a Lindblad term $\mathcal{L}[\rho] = -\rho L^\dagger L - L^\dagger L \rho + 2L\rho L^\dagger$, where

$$L = \begin{pmatrix} 1 & 0 \\ 0 & 0 \end{pmatrix}, \text{ so that the density matrix obeys}$$

$$\frac{d}{dt}\rho = -i[H, \rho] + \Gamma\mathcal{L}[\rho]. \quad (33)$$

Writing $\rho = \begin{pmatrix} \rho_{11} & e^{-it\omega_1}\rho_{12} \\ e^{it\omega_1}\rho_{21} & \rho_{22} \end{pmatrix}$, equations for the slowly evolving ρ_{ij} can be found by imposing the rotating

Decay Rate	Component
$-\frac{20\beta^2}{3\alpha}$	$\rho_{42} - \rho_{24}$ $\rho_{31} - \rho_{13}$
$-\frac{5\beta^2}{3\alpha}$	ρ_{84} ρ_{82} ρ_{73} ρ_{64} ρ_{53} ρ_{51} ρ_{48} ρ_{46} ρ_{37} ρ_{35} ρ_{28} ρ_{26} ρ_{17} ρ_{15}
$-\frac{5\beta^2}{3\alpha} + \frac{\beta^2}{9\kappa} - \frac{\beta}{18}$	$\rho_{26} + \rho_{71}$ $\rho_{17} + \rho_{62}$
$-\frac{20\beta^2}{3\alpha} + \frac{4\beta^2}{9\kappa} - \frac{2\beta}{9}$	$\rho_{44} - \rho_{22}$ $\rho_{33} - \rho_{11}$

TABLE VI. Decaying density matrix components and associated decay rates resulting from hyperfine interaction $H_0 = \alpha(\vec{I} \cdot \Delta\vec{S})$ and Zeeman interaction $V = H_z = \beta(S_{z1} + S_{z2})$ in the limit that $\beta \ll \alpha$. Indices are numbered according to Table II. Negative rates correspond to decay.

wave approximation $e^{in\omega_1 t} \rightarrow 0$ for $n \neq 0$, so that

$$\begin{pmatrix} \dot{\rho}_{11} \\ \dot{\rho}_{12} \\ \dot{\rho}_{21} \\ \dot{\rho}_{22} \end{pmatrix} = \begin{pmatrix} \frac{1}{2}ide^{it\Delta}\rho_{12} - \frac{1}{2}ide^{-it\Delta}\rho_{21} \\ \frac{1}{2}ide^{-it\Delta}\rho_{11} - \frac{1}{2}ide^{-it\Delta}\rho_{22} - \rho_{12}\Gamma \\ -\frac{1}{2}ide^{it\Delta}\rho_{11} + \frac{1}{2}ide^{it\Delta}\rho_{22} - \rho_{21}\Gamma \\ \frac{1}{2}ide^{-it\Delta}\rho_{21} - \frac{1}{2}ide^{it\Delta}\rho_{12} \end{pmatrix} \quad (34)$$

A second order differential equation for the density matrix components can now be found by taking the time derivative of Eq. 34, then using Eq. 34 to substitute for terms of the form $\dot{\rho}_{ij}$, yielding

$$\begin{pmatrix} \ddot{\rho}_{11} \\ \ddot{\rho}_{12} \\ \ddot{\rho}_{21} \\ \ddot{\rho}_{22} \end{pmatrix} = \begin{pmatrix} -\frac{\rho_{11}d^2}{2} + \frac{\rho_{22}d^2}{2} - \frac{1}{2}ie^{it\Delta}\rho_{12}\Gamma d + \frac{1}{2}ie^{-it\Delta}\rho_{21}\Gamma d - \frac{1}{2}e^{it\Delta}\rho_{12}\Delta d - \frac{1}{2}e^{-it\Delta}\rho_{21}\Delta d \\ -\frac{\rho_{12}d^2}{2} + \frac{1}{2}e^{-2it\Delta}\rho_{21}d^2 - \frac{1}{2}ie^{-it\Delta}\rho_{11}\Gamma d + \frac{1}{2}ie^{-it\Delta}\rho_{22}\Gamma d + \frac{1}{2}e^{-it\Delta}\rho_{11}\Delta d - \frac{1}{2}e^{-it\Delta}\rho_{22}\Delta d + \rho_{12}\Gamma^2 \\ \frac{1}{2}e^{2it\Delta}\rho_{12}d^2 - \frac{\rho_{21}d^2}{2} + \frac{1}{2}ie^{it\Delta}\rho_{11}\Gamma d - \frac{1}{2}ie^{it\Delta}\rho_{22}\Gamma d + \frac{1}{2}e^{it\Delta}\rho_{11}\Delta d - \frac{1}{2}e^{it\Delta}\rho_{22}\Delta d + \rho_{21}\Gamma^2 \\ \frac{\rho_{11}d^2}{2} - \frac{\rho_{22}d^2}{2} + \frac{1}{2}ie^{it\Delta}\rho_{12}\Gamma d - \frac{1}{2}ie^{-it\Delta}\rho_{21}\Gamma d + \frac{1}{2}e^{it\Delta}\rho_{12}\Delta d + \frac{1}{2}e^{-it\Delta}\rho_{21}\Delta d \end{pmatrix} \quad (35)$$

In the limit that $\Gamma \gg d$, terms of order Γ^2 dominate Eq. 35, so that ρ_{12} and ρ_{21} decay as $e^{-\Gamma t}$. Substituting $\rho_{12}, \rho_{21} \rightarrow 0$ into Eq. 35 yields a second order differential equation for the population difference

$$\ddot{\rho}_{11} - \ddot{\rho}_{22} = -d^2(\rho_{11} - \rho_{22}), \quad (36)$$

so that the population difference oscillates as

$$(\rho_{11}(t) - \rho_{22}(t)) = A \sin(dt) + B \cos(dt). \quad (37)$$

Note that the rapid decay of ρ_{12} and ρ_{21} cause terms involving Δ to vanish from the equation for the population difference, so that the effects of nonzero detuning are small in the limit of rapid dephasing.

For a radical pair in an initial singlet state, it is the difference $\Delta\mu$ between the effective magnetic moments of the two spins which drives spin flips. Using $H_0^{rP} = 1/2\Delta\mu\vec{B}\cdot\Delta\vec{S}$ from Eq. 2 in the body of the paper, the three states with $\Delta s = 1, \Delta m_s = -1, 0, 1$ are coupled by the oscillatory field according to $\frac{1}{2}B(t)\Delta\mu\sigma_x =$

$$\frac{B_{\text{osc}}\Delta\mu}{2\sqrt{2}} \cos(\omega_2 t) \begin{pmatrix} 0 & 1 & 0 \\ 1 & 0 & 1 \\ 0 & 1 & 0 \end{pmatrix}. \quad \text{Setting } \Delta\mu = 1 \text{ as in the}$$

body of the paper yields $d = \frac{B_{\text{osc}}}{2\sqrt{2}}$ for both of the two Rabi pathways.

-
- [1] W. Wiltschko and R. Wiltschko, *Journal of Comparative Physiology A: Neuroethology, Sensory, Neural, and Behavioral Physiology* **191**, 675 (2005).
- [2] R. Muheim, *Photobiology*, 465 (2008).
- [3] R. Wiltschko, I. Schiffner, P. Fuhrmann, and W. Wiltschko, *Current Biology* **20**, 1534 (2010).
- [4] L. Wu and J. Dickman, *Current Biology* (2011).
- [5] L. Wu and J. Dickman, *Science* (2012).
- [6] C. D. Treiber, M. C. Salzer, J. Riegler, N. Edelman, C. Sugar, M. Breuss, P. Pichler, H. Cadiou, M. Saunders, M. Lythgoe, *et al.*, *Nature* (2012).
- [7] W. Wiltschko, R. Wiltschko, and T. Ritz, *Procedia Chemistry* **3**, 276 (2011).
- [8] T. Ritz, *Procedia Chemistry* **3**, 262 (2011).
- [9] S. Johnsen and K. Lohmann, *Nature Reviews Neuroscience* **6**, 703 (2005).
- [10] K. Able, *The condor* **97**, 592 (1995).
- [11] W. Beck and W. Wiltschko, *Behaviour*, 145 (1983).
- [12] R. Muheim, J. Bäckman, and S. Åkesson, *Journal of Experimental Biology* **205**, 3845 (2002).
- [13] W. Wiltschko, R. Wiltschko, *et al.*, *Science* **176**, 62 (1972).
- [14] T. Ritz, R. Wiltschko, P. Hore, C. Rodgers, K. Stapput, P. Thalau, C. Timmel, and W. Wiltschko, *Biophysical Journal* **96**, 3451 (2009).
- [15] T. Ritz, P. Thalau, J. Phillips, R. Wiltschko, and W. Wiltschko, *Nature* **429**, 177 (2004).
- [16] K. Schulten, C. Swenberg, and A. Weller, *Zeitschrift für Physikalische Chemie* **111**, 1 (1978).
- [17] T. Ritz, S. Adem, and K. Schulten, *Biophysical Journal* **78**, 707 (2000).
- [18] A. M. Stoneham, E. M. Gauger, K. Porfyraakis, S. C. Benjamin, and B. W. Lovett, *Biophysical Journal* **102**, 961 (2012).
- [19] A. L. Buchachenko, *Russian Chemical Reviews* **83**, 1 (2014).
- [20] E. M. Gauger, E. Rieper, J. J. Morton, S. C. Benjamin, and V. Vedral, *Physical review letters* **106**, 40503 (2011).
- [21] J. Bandyopadhyay, T. Paterek, and D. Kaszlikowski, *Physical Review Letters* **109**, 110502 (2012).
- [22] E. Gauger and S. C. Benjamin, *Physical Review Letters* **110**, 178901 (2013).
- [23] J. Bandyopadhyay, T. Paterek, and D. Kaszlikowski, *Physical Review Letters* **110**, 178902 (2013).
- [24] I. Kominis *et al.*, *Physical Review-Section E-Statistical Nonlinear and Soft Matter Physics* **80**, 56115 (2009).
- [25] J. Jones and P. Hore, *Chemical Physics Letters* **488**, 90 (2010).
- [26] I. Kominis, *Physical Review E* **83**, 056118 (2011).
- [27] A. Dellis and I. Kominis, *Biosystems* (2011).
- [28] K. Kavokin, *Bioelectromagnetics* **30**, 402 (2009).
- [29] J. Cai, G. Guerreschi, and H. Briegel, *Physical review letters* **104**, 220502 (2010).
- [30] M. Tiersch and H. J. Briegel, *Philosophical Transactions of the Royal Society A: Mathematical, Physical and Engineering Sciences* **370**, 4517 (2012).
- [31] J. Cai, F. Caruso, and M. Plenio, *Physical Review A* **85**, 040304 (2012).
- [32] A. Johnson, J. Petta, J. Taylor, A. Yacoby, M. Lukin, C. Marcus, M. Hanson, and A. Gossard, *Nature* **435**, 925 (2005).
- [33] J. Petta, A. Johnson, J. Taylor, E. Laird, A. Yacoby, M. Lukin, C. Marcus, M. Hanson, and A. Gossard, *Science* **309**, 2180 (2005).
- [34] J. Cai, *Physical Review Letters* **106**, 100501 (2011).
- [35] C. Cai, Q. Ai, H. Quan, and C. Sun, *Physical Review A* **85**, 022315 (2012).
- [36] M. Liedvogel and H. Mouritsen, *Journal of The Royal Society Interface* **7**, S147 (2010).
- [37] H. Hogben, O. Efimova, N. Wagner-Rundell, C. Timmel, and P. Hore, *Chemical Physics Letters* **480**, 118 (2009).
- [38] C. Nießner, S. Denzau, J. Gross, L. Peichl, H. Bischof, G. Fleissner, W. Wiltschko, and R. Wiltschko, *PLoS one* **6**, e20091 (2011).
- [39] D. Home and M. Whitaker, *Annals of Physics* **258**, 237 (1997).
- [40] Z. Walters, *Quantum Physics Letters* **1**, 21 (2012).

- [41] W. Wiltschko, K. Stapput, P. Thalau, and R. Wiltschko, *Naturwissenschaften* **93**, 300 (2006).
- [42] M. A. Schlosshauer, *Decoherence and the quantum-to-classical transition* (Springer, 2007).
- [43] A. Bandrauk and H. Shen, *Chemical physics letters* **176**, 428 (1991).
- [44] K. Blum, *Density matrix theory and applications* (Springer, 2012).
- [45] G. Woodgate, *Elementary atomic structure* (Oxford University Press, USA, 1983).